

Flatness measurement by scanning deflectometric profiler

Yohan Kondo¹⁾ and Youichi Bitou¹⁾

¹ Length Standards Group, National Metrology Institute of Japan, National Institute of Advanced Industrial Science and Technology (NMIJ/AIST)

kondou.y@aist.go.jp

Abstract

The Fizeau interferometer is highly accurate surface profile measurement system, however; it is difficult to obtain the absolute surface profile because it is a comparison measurement with a reference surface. When a measurement direction is parallel to the gravity direction, a gravity deformation of a reference surface is a large uncertainty component. In this study, we developed an absolute surface profiler based on the local slope angle measurement of the specimen without using the reference surface, which is called the scanning deflectometric profiler (SDP). Measuring devices based on deflectometry have been developed by many laboratories as a highly accurate straightness profile measurement. On the other hand, a problem of deflectometric system was that the measurement was limited to a line (two-dimensional) profile. To solve this problem, we developed a novel method to measure the surface topography. The surface topography was calculated from radial lines obtained by rotating the specimen. In this paper, we performed the comparison measurement between the SDP system and the Fizeau interferometer. Finally, the proposed method was validated through the comparison measurement.

Flatness, Surface topography, Deflectometry, Angle, Fizeau interferometer

1. Introduction

The Fizeau interferometer is highly accurate surface profile measurement system, however; it is difficult to obtain the absolute surface profile because it is a comparison measurement with a reference surface. When a measurement direction is parallel to the gravity direction, the gravity deformation of a reference surface is a large uncertainty component. In recent years, a highly accurate surface profile measurement methods based on angle measurement which is called deflectometry have attracted attention [1-10]. In this method, a local slope angle distribution on a specimen is measured by scanning a pentamirror using an autocollimator, and a surface profile is obtained by integrating the obtained local slope angle distribution. Unlike the case of the Fizeau interferometer, deflectometric method has characteristics that it does not require a reference surface and can directly measure a large-diameter surface profile. On the other hand, there is a problem that the measurement is limited to a line (two-dimensional) profile. In this study, we developed a novel method based on the deflectometry to measure the surface topography.

2. Line profile measurement [10]

In a previous study [10], we developed a scanning deflectometric profiler (SDP) that does not require a reference flat and can directly measure a surface profile. The system within the dotted line in figure 1 is a schematic view of the developed SDP. The SDP is constructed using an autocollimator and a pentamirror fixed on an air slide table. The travel distance of the air slide table is 1.2 m. The measurement beam of the autocollimator is bent by the pentamirror so that it illuminates a specimen. The optical system of the SDP is aligned according to the literatures [11-13] of an alignment procedure for a deflectometry system. The size of the measurement beam is $\Phi 34$ mm. An aperture is set in front of the specimen for

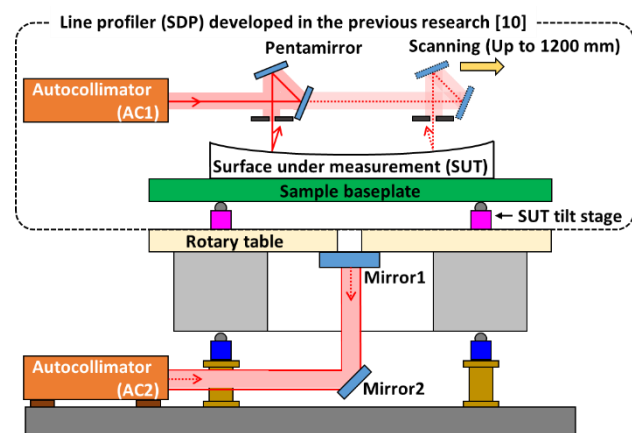


Figure 1. Schematic view of the 3-D SDP.

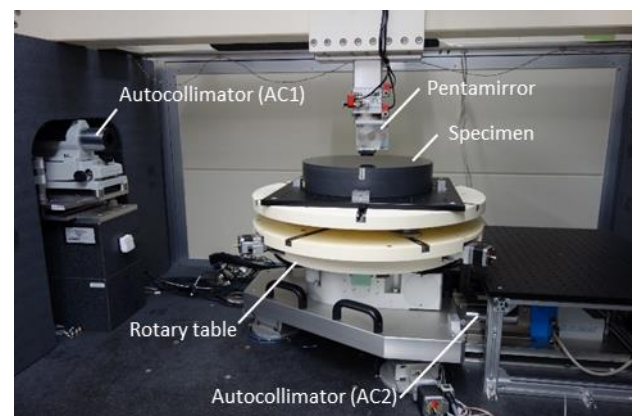


Figure 2. Photograph of the 3-D SDP.

increasing the special frequency. Local slope angles at each position of the specimen are measured by scanning the pentamirror. The pentamirror is effective for minimizing the moving error during scanning, and the influence of the moving error on the local slope angle measurement is negligible [11-13]. The surface profile $F(x_i)$ of the specimen is obtained by integrating the local slope angles as follows:

$$f(x_i) = 0 \quad (i = 1) \quad (1)$$

$$f(x_i) = f(x_{i-1}) + \{f'(x_i) - f'(x_{i-1})\}(x_i - x_{i-1}) \quad (i = 2, 3, \dots, N), \quad (2)$$

where i is a measurement number, N is a total number of measurement points, $f(x_i)$ is a profile, $f'(x_i)$ is a measured local slope angle and x_i is measurement position. The measured slope angle $f'(x_1)$ of the first measurement position x_1 can be selected an arbitrary angle. The numerical integration of Eqs. (1) and (2) is calculated that the measured angle of the first measurement position is be zero. An DC component a_0 of the measured slope angle $f'(x_i)$ is be a line $g(x_i) = a_0 x_i + b$. Then, the least-squares line $g(x_i)$ is calculated from the profile $f(x_i)$. By subtracted $g(x_i)$ from $f(x_i)$, we can obtain the final profile $F(x_i)$ as follows:

$$F(x_i) = f(x_i) - g(x_i). \quad (3)$$

We used a commercial autocollimator (MÖLLER-WEDEL OPTICAL GmbH, ELCOMAT 3000) of which the total measurement range and the resolution are ± 1000 (5.1 mrad) arcsec and 0.001 (4.8 nrad) arcsec, respectively. The measurement accuracy of the autocollimator is the most important aspect of the SDP based on the angle measurement. The autocollimator static stability and systematic error were evaluated using a high accuracy angle index table at National Metrology Institute of Japan (NMIJ/AIST) [14]. The measurement accuracy of the rotation angle of the index table is less than 0.005 arcsec (24.2 nrad).

For short-term stability, the standard deviation of the autocollimator was 0.008 arcsec (38.9 nrad) when the sampling rate and the number of measurement points were 25 Hz and 100 points, respectively. As a surface profile is calculated by integrating the local slope angles at each measurement position, the random error is also integrated. The standard uncertainty u_{rand} of the random error is given by

$$u_{\text{rand}} = \sigma_{\text{rand}} \cdot \sqrt{N} dx, \quad (4)$$

where N and dx are the total number of measurement points and the scanning pitch, respectively. When N and dx are 300 points and 1 mm, respectively, the standard uncertainty is 0.67 nm. The final profile $F(x_i)$ is obtained by subtracted an DC component of measured angle slope $f'(x_i)$ from Eq. (3); therefore, an DC component of an integrated random error is also subtracted. Eq. (4) is overestimate but the expected value of the random error is zero and the overestimate value is very small.

In this study, the measurement surface is an optical flat with a flatness of about $\lambda / 2$ (316.4 nm) or less. The measurement range of the autocollimator is very small. The systematic error of the autocollimator was evaluated in the range of ± 5 arcsec ($\pm 24.2 \mu\text{rad}$). For systematic error, the maximum deviation e_a of the angle over the range of evaluation (P-V value) was 0.032 arcsec (155.1 nrad). The measurement range of the autocollimator varies with the surface profile of the specimen. We assume that the standard deviation of the systematic error is set to be the uniform distribution of the maximum angle deviation of the calibration curve, then the standard uncertainty u_{sys} of the systematic error is given by

$$u_{\text{sys}} = \frac{e_a}{2\sqrt{3}} \cdot \sqrt{N} dx. \quad (5)$$

N and dx are 300 points and 1 mm, respectively, the standard uncertainty is 0.78 nm.

3. Surface topography measurement method

The SDP is a line profiler that can measure with a few nanometers uncertainty. On the other hand, the problem of SDP system is that the measurement is limited to a line (two-dimensional) profile. To solve this problem, we developed a novel method to measure the surface topography. Figure 1 and 2 show a schematic view and a photograph of the developed profiler which is called 3-D scanning deflectometric profiler (3-D SDP). A rotary stage was introduced to the sample stage of the line profiler (SDP) developed in the previous research [10]. By rotating the specimen, radial line profile measurements are performed, and a surface topography is obtained by connecting each line profile; however, the relative angle relationship between the line profiles is not clear due to the angular runout of the rotary stage.

To solve this problem, we measured circumference profiles in addition to the line profile measurements (see figure 3). In the circumference profile measurement, the pentamirror is moved to a certain radial position from the center of rotation, and the autocollimator measures a local slope angle of the specimen of a component orthogonal to the scanning axis of the pentamirror. The local slope angle distribution is measured by rotating the specimen and a circumference profile is obtained by integrating the obtained local slope angle distribution. However, the measurement result includes an angular runout of the rotary stage. To remove the runout, a mirror 1 is set in the center of the back surface of the sample table, and the angular runout is corrected using another autocollimator AC2 (see figure 1). Finally, the relative angle relationship can be determined from the intersection data of the radial line profiles and the circumferential profiles.

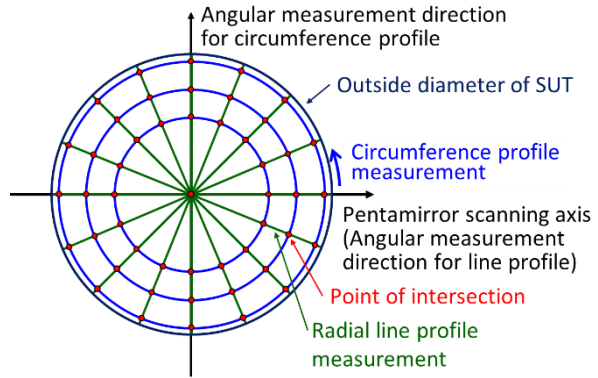


Figure 3. Systematic view of connection of each profile measurement

4. Experiment

We measured the flatness of an optical flat using the developed 3-D SDP. The optical flat is 340 mm in diameter and 70 mm in thickness, and is made of the ultralow-expansion ceramic NEXCERA™. The evaluation range of the surface topography is 300 mm in diameter. Figure 4 shows the measurement procedure of the surface topography of the optical flat. The details of each step are described below.

(a) Adjustment of pentamirror

The optical axis of the autocollimator was adjusted to be parallel to the axis of motion of the air slide. Then, the pentamirror was aligned according to the literatures [11-13] of

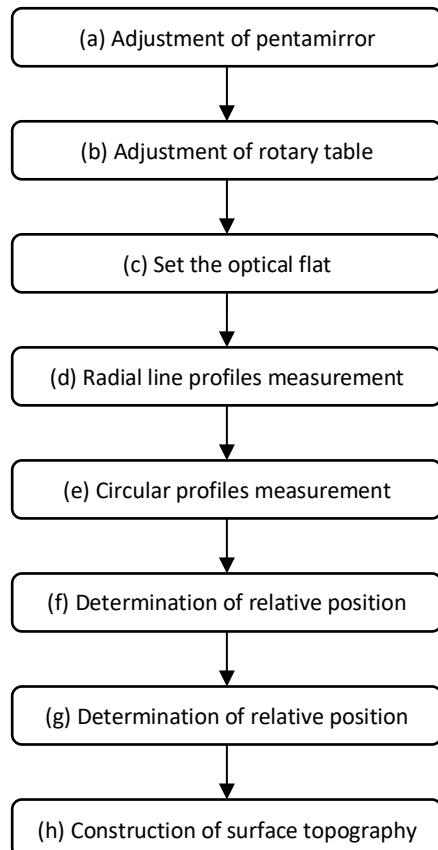


Figure 4. Measurement procedure of surface topography

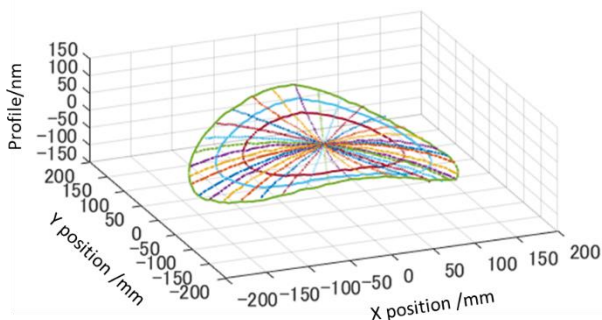


Figure 5. Radial and circumferential measurement profiles

pentamirror was aligned according to the literatures [11-13] of an alignment procedure for a deflectometry system.

(b) Adjustment of rotary table

The position of the rotary table was adjusted so that the measurement beam (Z-axis) passing through the aperture passed through the center of rotation of the rotary table. The adjustment method is as follows.

The misalignment between the measurement beam of the autocollimator and the center of rotation of the rotary table was detected using a quadrant photodiode detector (QPD). The QPD was set on the rotary table so that the center of the QPD coincided with the rotation center of the rotary stage. If there is misalignment between the measurement beam of the autocollimator and the center of rotation of the rotary table, the trajectory of the QPD signal draws a circle when the rotary table is rotated. The displacement in the pentamirror scanning axis direction (X-axis) between of the center of rotation of the rotary table and the measurement beam of the autocollimator was adjusted by moving the pentamirror. The displacement in the direction (Y-axis) orthogonal to the pentamirror scanning axis

between the center of rotation of the rotary table and the measurement beam of the autocollimator was adjusted by moving the rotary table. For the adjustment value, the deviation between the center of rotation of the rotary table and the measurement beam of the autocollimator was adjusted to 50 μm or less. This adjustment error causes a position error when connecting the radial line profiles and the circumference profiles. The effect, however, is very small because a specimen in our target has a very smooth surface. If the measurement surface is not flat, for example a spherical surface and a paraboloidal surface, this effect must be noted.

(c) Set the optical flat

The optical flat was set on the rotary stage. The optical flat was arranged so that the center of the optical flat coincided with the rotation center of the rotary stage. In the 3-D SDP, the center of the workpiece coordinate system of the specimen is the center of rotation of the rotary stage. The center of the optical flat was adjusted using a displacement sensor so that the radial runout of the outer circumference of the optical flat was 10 μm or less.

(d) Radial line profiles measurement

A line profile measurement in a 300 mm range was performed in 1 mm steps. Then, the specimen was rotated 10 degrees, and the line profile was measured in the same manner. This step was repeated to obtain a total of 18-line profiles.

(e) Circular profiles measurement

The circumference profiles were measured in 1-degree steps at the positions of the radii $r = 150$ mm, 120 mm and 90 mm. The rotation angle was measured by a rotary encoder.

(f) Determination of relative position of radial line profiles

The relative angle of each radial line profile was determined from a circular profile with a radius $r = 150$ mm. At the intersection of two points of the radial line profiles and the circumference profile, the inclination angle of each radial line profile was determined from the distance between the two points (300 mm) and the profile deviation value between the two points of the circumference profile. The height of each radial line profile was determined by setting the common center coordinate to zero $(x, y, z) = (0, 0, 0)$.

(g) Determination of relative position of circular profiles

The relative angular relationship of each circumference profile is also unknown. The relative angle of each circumference profile was determined from the already determined radial line profiles. For the radial profiles, the points at the intersection with each circumference profile were extracted. In this case, there are 36 points for each circumference profile. A normal vector of the least-squares plane was calculated from the point cloud data extracted from the radial line profiles. In the same manner, a normal vector of the least-squares plane is calculated from the point cloud data extracted from a circumference profile. The circumference profile was rotated about the X-axis and the Y-axis so that the normal vector calculated from the circumference profile coincided with the normal vector calculated from the radial line profile. The height in the Z direction of the circumference profile was determined so that the average Z coordinate of the extracted circumference profile and the average Z coordinate of the extracted radial line profiles became equal.

(h) Construction of surface topography

Figure 4 shows the obtained radial line profiles and the circumference profiles according to the above procedure (a) to

(g). Figure 5 shows the surface topography with a diameter of 300 mm which is constructed from the obtained profiles by Zernike polynomial of the 36th order. The peak-to-valley (P-V) value, that is, the flatness and the root mean square (RMS) value were 131.7 nm and 26.0 nm, respectively.

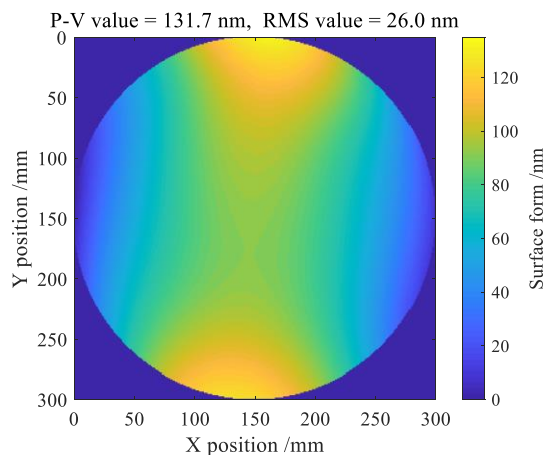


Figure 6. Surface topography by 3D-SDP

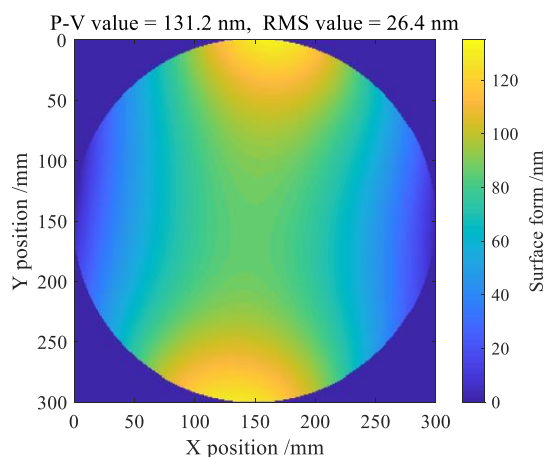


Figure 7. Surface topography by Fizeau interferometer

To verify the proposed method, we performed a comparative measurement of same optical flat using Fizeau flatness interferometer owned by the National Metrology Institute of Japan (NMIJ/AIST). Its measurement range and measurement uncertainty of flatness are 300 mm and 10 nm ($k = 2$), respectively. Figure 6 shows the measurement result. The P-V value and the RMS value were 131.2 nm and 26.4 nm, respectively. Both results are in good agreement despite different methods.

5. Conclusion

We proposed the topography measurement based on the deflectometry. Deflectometric profiler has previously been limited to line (two-dimensional) profile measurement. In this study, the surface topography measurement was realized by combining radial and circumferential profile measurements. In the future, we will clarify the factors of measurement uncertainty of the 3-D SDP.

Acknowledgement

This work was supported by JSPS KAKENHI Grant Numbers JP17H04901, JP.26820028 and Mitutoyo association for science and technology (MAST).

References

- [1] R. D. Geckeler and I. Weingärtner, "Sub-nm Topography Measurement by Deflectometry: Flatness Standard and Wafer Nanotopography" Proc. SPIE, 4779, 1-12, 2002.
- [2] F. Siewert, J. Buchheim and T. Zeschke, "Characterization and calibration of 2nd generation slope measuring profiler" Nucl. Instrum. Methods in Phys. Res. A, 616(2-3), 119-127, 2010.
- [3] M. Schulz, G. Ehret, M. Stavridis and C. Elster, "Concept, design and capability analysis of the new Deflectometric Flatness Reference at PTB" Nucl. Instrum. Methods Phys. Res. A, 616(2-3), 134-139, 2010.
- [4] V. V. Yashchuk, S. Barber, E. E. Domning, J. L. Kirschman, G. Y. Morrison, B. V. Smith, F. Siewert, T. Zeschke, R. Geckeler and A. Just, "Sub-microradian surface slope metrology with the ALS Developmental Long Trace Profiler" Nucl. Instrum. Methods Phys. Res. A, 616(2-3), 212-223, 2010.
- [5] S. G. Alcock, K. J. S. Sawhney, S. Scott, U. Pedersen, R. Walton, F. Siewert, T. Zeschke, F. Senf, T. Noll and H. Lammert, "The Diamond-NOM: A non-contact profiler capable of characterizing optical figure error with sub-nanometre repeatability" Nucl. Instrum. Methods Phys. Res. A, 616(2-3), 224-228, 2010.
- [6] Y. Senba, H. Kishimoto, H. Ohashi, H. Yumoto, T. Zeschke, F. Siewert, S. Goto and T. Ishikawa, "Upgrade of long trace profiler for characterization of high-precision X-ray mirrors at SPring-8" Nucl. Instrum. Methods Phys. Res. A, 616(2-3), 237-240, 2010.
- [7] M. Xiao, S. Jujo, S. Takahashi and K. Takamasu, "Nanometer profile measurement of large aspheric optics surface by scanning deflectometry with rotatable devices: Uncertainty propagation analysis and experiments" Prec. Eng., 36(1), 91-96, 2012.
- [8] G. Ehret, M. Schulz, M. Stavridis and C. Elster, "Deflectometric system for absolute flatness measurements at PTB" Meas. Sci. Technol., 23(9), 094007(8pp), 2012.
- [9] G. Ehret, M. Schulz, M. Baier and A. Fitzenreiter, "Optical measurement of absolute flatness with the deflectometric measurement systems at PTB" J. Phys.: Conf. Ser., 425(15), 152016 (4pp), 2013.
- [10] Y. Kondo and Y. Bitou, "Evaluation of deformation value of optical flat under gravity" Meas. Sci. Technol., 25(6), 064007 (8pp), 2014
- [11] R. D. Geckeler, "Optimal use of pentaprisms in highly accurate deflectometric scanning" Meas. Sci. Technol., 18(1), 115-125, 2007.
- [12] G. Ehret, M. Schulz, A. Fitzenreiter, M. Baier, W. Jöckel, M Stavridis and C. Elster, "Alignment methods for ultraprecise deflectometric flatness metrology" Proc. SPIE, 8082, 808213, 2011.
- [13] S. B. Samuel, R. D. Geckeler, V. V. Yashchuk, M. V. Gubarev M V, J. Buchheim, F. Siewert and T. Zeschke, "Optimal alignment of mirror-based pentaprisms for scanning deflectometric devices" Opt. Eng., 50(7), 073602(8pp), 2011.
- [14] T. Watanabe and H. Fujimoto, "High accuracy angle indexing table" Proc. XIVIII IMEKO World Congress, 2006.